Magn Reson Med Sci 2018; 17; 308–317
doi:10.2463/mrms.mp.2017-0100
Published Online: February 21, 2018

MAJOR PAPER

Evaluation of a Portable Doppler Ultrasound Gating Device for Fetal Cardiac MR Imaging: Initial Results at 1.5T and 3T

Fabian Kording[1,2*], Bjoern P. Schoennagel[1], Manuela Tavares de Sousa[3], Kai Fehrs[1,2], Gerhard Adam[1], Jin Yamamura[1], and Christian Ruprecht[1,2]

Purpose: Fetal cardiac MRI has the potential to play an important role in the assessment of fetal cardiac pathologies, but it is up to now not feasible due to a missing gating method. The purpose of this work was the evaluation of Doppler ultrasound (DUS) for external fetal cardiac gating with regard to compatibility, functionality, and reliability. Preliminary results were assessed performing fetal cardiac MRI.

Methods: An MRI conditional DUS device was developed to obtain a gating signal from the fetal heart. The MRI compatibility was evaluated at 1.5T and 3T using B_1 field maps and gradient echo images. The quality and sensitivity of the DUS device to detect the fetal heart motion for cardiac gating were evaluated outside the MRI room in 15 fetuses. A dynamic fetal cardiac phantom was employed to evaluate distortions of the DUS device and gating signal due to electromagnetic interferences at 1.5T and 3T. In the first *in vivo* experience, dynamic fetal cardiac images were acquired in four-chamber view at 1.5T and 3T in two fetuses.

Results: The maximum change in the B_1 field and signal intensity with and without the DUS device was <6.5% for 1.5T and 3T. The sensitivity of the DUS device to detect the fetal heartbeat was 99.1%. Validation of the DUS device using the fetal cardiac phantom revealed no electromagnetic interferences at 1.5T or 3T and a high correlation to the simulated heart frequencies. Fetal cardiac cine images were successfully applied and showed good image quality.

Conclusion: An MR conditional DUS gating device was developed and evaluated revealing safety, compatibility, and reliability for different field strengths. In a preliminary experience, the DUS device was successfully applied for *in vivo* fetal cardiac imaging at 1.5T and 3T.

Keywords: *magnetic resonance imaging, cardiovascular system, fetal heart, Doppler ultrasound*

Introduction

The imaging modality of choice for prenatal diagnosis of congenital heart disease (CHD) is due to its ease of use, high availability, and high diagnostic accuracy fetal echocardiography.[1,2] However, fetal echocardiography is occasionally limited by the acoustic window, fetal position, maternal adipose tissue, gestational age, abdominal wall scars, and the level of training of the operator.[3,4]

Prenatal detection of CHD using echocardiography varies widely from 13% to 82%.[5] Moreover, discordances of up to 29% between pre- and post-natal diagnoses of CHD and a limited ability to measure blood flow using echocardiography encourages the development of new techniques to improve prenatal cardiovascular imaging.[6]

Fetal MRI is increasingly used as a second-line imaging tool for prenatal evaluation of the fetal brain[7] and other organs including the fetal heart.[3] Fetal cardiac MRI may provide a valuable adjunct to fetal echocardiography as it provides the ability to image the fetal heart with excellent tissue contrast in arbitrary planes independent of the above-mentioned limitations of fetal echocardiography.[8] Fetal cardiovascular magnetic resonance (CMR) may be especially helpful for the detection of duct-dependent lesions, such as coarctation of the aorta[9] and to recognize CHD in late gestation.[3] One of the main challenges for high-quality fetal cardiac images using conventional cine reconstruction methods is accurate synchronization of the cardiac cycle with the MRI data acquisition,[10] usually achieved using the spatial information of an electrocardiogram (ECG).[11] However, the ECG cannot be applied for fetal cardiac MRI and

[1]Department of Diagnostic and Interventional Radiology and Nuclear Medicine, University Medical Center Hamburg-Eppendorf, Martinistraße 52, 20246 Hamburg, Germany
[2]northh medical GmbH, Hamburg, Germany
[3]Department of Obstetrics and Fetal Medicine, University Medical Center Hamburg-Eppendorf, Hamburg, Germany
*Corresponding author, Phone: +49-40-7410-58152,
E-mail: f.kording@uke.de

Received: July 28, 2017 | Accepted: December 20, 2017

several methods were developed to assign the acquired image data to the correct cardiac cycle using retrospective image reconstruction based on post-processing techniques.[12–14] Although post-processing methods are capable of producing a good image quality, their time-consuming image reconstruction in combination with fetal movement represents a crucial disadvantage and prevents the possibility to adapt imaging planes in real time.

In order to employ clinically proven cardiac imaging methods in conjunction with an immediate image reconstruction, a direct gating method is necessary. A well-established technique to acquire the fetal heart rate is based on Doppler ultrasound (DUS).[15] Doppler ultrasound is capable of recording the fetal heart rate in real-time and is in theory not influenced by the electromagnetic field of the MRI.[16–18] Thus, DUS represents an ideal method to synchronize the MRI data acquisition with the fetal cardiac cycle. The method was applied to gate the image acquisition for adult cardiac MRI[19,20] and for fetal MRI in a sheep model[21] using a standard cardiotocograph (CTG). However, using a commercially available CTG is accompanied by two major drawbacks. First, the software is not designed to detect every single heartbeat of the fetus, which is implicitly necessary for cardiac cine MRI. Second, the hardware is normally not designed for the hazardous MRI environment, e.g., regarding safety concerns by placing the transducer and connecting cable directly under the Receive (RX) coil.

The purpose of this work was to develop and evaluate an MRI conditional and portable DUS device for 1.5T and 3T that can be operated within the MRI room during image acquisition with regard on compatibility, functionality, and reliability in order to enable fetal cardiac gating for cine MRI.

Materials and Methods

Study population

The study population consisted of 15 healthy pregnant volunteers (30–37 weeks gestation) participating in the validation study outside the MRI and two healthy pregnant volunteers for the MRI measurements (34 and 36 weeks of gestation). The fetuses of the pregnant volunteers had no diagnosis or suspicion of congenital cardiovascular disease. The study was approved by the local ethics committee. Informed written consent from each volunteer was obtained in advance of the study.

DUS gating device

The DUS gating setup is schematically shown in Fig. 1. The electronics of the DUS device was a custom build and was placed inside the MRI room during data acquisition. The DUS device was battery powered by lithium battery of 10.4 V with dimensions of $20 \times 10 \times 15$ cm^3. Ultrasound pulses of 1 MHz were transmitted with a repetition frequency of 3.2 kHz resulting in an acoustic intensity of 4.6 mW/cm^2 at the ultrasound transducer (HP 15245A; Hewlett Packard, Palo Alto, CA, USA). All components of the transducer were replaced by non-magnetic materials or materials with a low magnetic permeability. The piezoelectric elements were made of non-magnetic lead zirconate titanate with a diameter of 1 cm. The connection between the transducer and the DUS electronic was realized using a 7 m long cable shielded with aluminum. In order to ensure patient safety and sufficient MRI compatibility, the cable was decoupled with respect to the B_1 field using cable traps. As the DUS device was used at 1.5T and 3T, two different cable setups were used. Four cable traps were required for each cable with a distance of 30 cm for 1.5T and a distance of 20 cm at 3T.

A solenoid balun was used as cable trap for 64 MHz as described by Peterson et al.[22] and a floating shield current suppression trap was used for 128 MHz following the method of Seeber et al.[23] Each trap was tuned manually to the corresponding Larmor frequency using a network analyzer with a 50 Ω termination.

To create a gating signal, the received ultrasound signal was amplified in a first stage and demodulated and filtered in a second stage (Fig. 1) with a pass band of 0–400 Hz. The main components in the DUS signal are the heart wall motion and a fraction of the blood flow. The heart wall motion is more prominent than the blood flow[24] and consists mainly of the atrial and ventricular contraction.[25] The heart wall motion was chosen as a signal source for the Doppler signal as it directly reflects the moments in the time needed to synchronize the MRI. In order to exclude the blood flow, the Doppler signal was low-pass filtered with a cut-off frequency of 100 Hz. Subsequently, the envelope of the DUS signal (0–10 Hz) was used for further peak detection analysis implemented on a microcontroller (Fig. 1). The signal was evaluated in two different paths. A threshold was calculated based on the envelope of the DUS signal in order to exclude peaks related to myocardial motion during diastole. In parallel, an autocorrelation of the first 1250 ms of the DUS signal was performed to estimate the RR interval. In the following step, a shiftable cover window was calculated based on the estimated beat-to-beat (RR) interval and previously detected gating time points in order to restrict the peak detection to a time point where the next gating is expected (Fig. 1). Following, the peak detection was only performed inside the cover window and to peaks belonging to minima of the DUS signal. Based on the results of the last digital processing step, standard transistor–transistor logic (TTL) square wave gating signals were transferred to the MRI using a coaxial cable.

MRI safety

As long as conducting wires with a cable shield were used for signal transmission, the used transmission line can couple significantly with the transmitted energy of the radiofrequency (RF) transmit (TX) coil, leading to potentially large common mode currents associated with possible tissue burns along the cable.[26] Therefore, the cables were tested for MRI safety compliance. The ability to attenuate common mode currents and to decouple the cable from the RF transmit field was

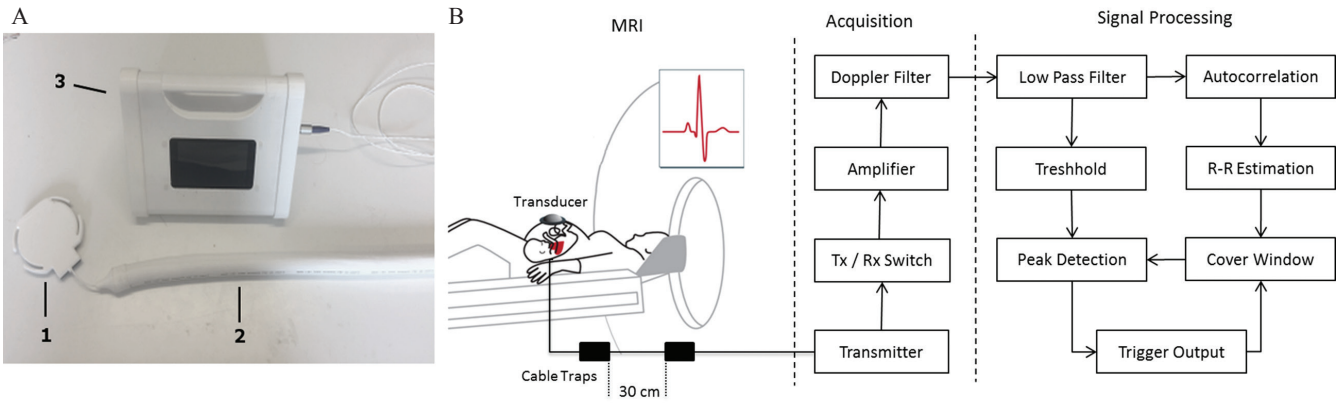

Fig. 1 (**A**) Used Doppler ultrasound (DUS) system with the ultrasound transducer (1) connected to the transmission line containing the cable traps, which are covered by a surrounding isolating sleeve (2). The ultrasound transducer is finally connected to the DUS device (3). The application of the DUS device to derive a fetal cardiac gating signal is shown schematically in (**B**). The transducer is placed above the fetal heart and is connected with the DUS electronic via a cable including cable traps to attenuate radiofrequency (RF) interferences. After signal acquisition, the signal processing algorithm is outlined schematically. The gating output is finally connected to the physiologic unit of the MRI.

evaluated using the 2-port transmission characteristics of S21 utilizing a network analyser (S332E Site Masters; Anritsu Corporation, Kanagawa, Japan) and current probes.

Moreover, the effect of the cable traps on the shield currents was tested using the method of Seeber et al.,[23] comparing the image homogeneity of large FOV (500 mm) coronal gradient echo images with and without the cable and transducer. Coronal views were chosen to show that there were no signal alterations along the cable due to common mode currents. For the measurement, two phantom bottles were placed next to each other with the cable in between. If common mode currents are present, image homogeneity will be affected by the shield currents leading to image distortions. Hence, the signal intensity within the phantom bottles was compared between images with and without transmission line. In addition, B_1 flip angle maps were acquired using a large water phantom filled with tissue simulating liquid in order to evaluate possible B_1 distortions due to inductive coupling with the transmission line.

Evaluation using a fetal cardiac phantom

The DUS device was first evaluated using a self-manufactured fetal cardiac phantom based on a simplified biventricular design (Fig. 2). The anatomical dimensions were based on literature values of a 36-week-old fetus with a right and left ventricular diameter of 215 mm and height of 590 mm.[27] A two-chamber structure polyamide mold was designed using a CAD software (Inventor; Autodesk Inc., San Rafael, CA, USA) and subsequently 3-D printed (Ultimaker, Geldermalsen, The Netherlands). For fabrication of the phantom, a room temperature vulcanization silicone rubber (TFC Silikon; Troll Factory Rainer Habekost e.K., Germany) was poured inside the mold with a cure time of 4 h. The heart was mounted in a sealed water container and connected to a hydraulic pumping system. The pulsatile flow was generated by an hydro-motor (Pentair / SHURFLO, Costa Mesa, CA, US) connected to two solenoid valves (NC

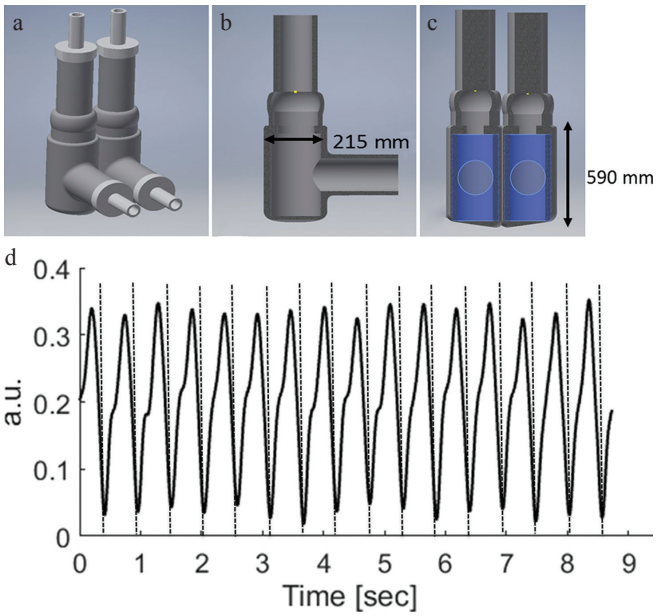

Fig. 2 The setup and dimensions of the used biventricular heart phantom are shown in (**a**–**c**). An example of the measured Doppler ultrasound signal from the moving heart phantom mimicking fetal heart movement is shown in (**d**) with corresponding detected gating signals (BPM = 118).

3/2; M&M International, Milano, Italy), controlled by a microcontroller (UNO AG; Arduino, Italy) that simulates the cardiac heart cycle.

In order to test the DUS device inside the MRI, the cardiac phantom was placed inside the 1.5T and 3T system and was connected to the pumping system that was placed outside of the MRI room. The DUS sensor was placed on the side of the water container to record the movement of the fetal heart phantom. The gating signal of the DUS device was subsequently transferred to the physiologic unit of the MRI

to test the ability of the DUS device to gate the heart movement using a steady-state free precession (SSFP) cine sequence at 1.5T and 3T. The frequency of the heart cycle was varied between 75 and 200 BPM in 20 steps and compared to the detected gating signal of the DUS device. Imaging parameters for 1.5T were: pixel spacing = 1.48 × 1.48 mm^2, slice thickness = 4 mm, TR = 3.1 ms, TE = 1.5 ms, flip-angle = 60°, parallel acquisition technique = sensitivity encoding (SENSE) (acceleration factor = 2), matrix = 256 × 256, phases = 30, slices = 20, temporal resolution = 30 ms, and for 3T: pixel spacing = 0.99 × 0.99 mm^2 matrix: 352 × 352, TR = 4.8 ms, TE = 1.4 ms, flip-angle = 45°, turbo factor = 13, SENSE = 2, slices = 8, slice thickness = 4 mm.

Verification of the DUS algorithm

The proposed algorithm to detect the fetal heart motion was evaluated prior to MRI measurements in the department of gynecology outside the MRI at 15 pregnant volunteers at 29–39 weeks of gestation. The transducer of the DUS device was placed above the fetal heart on the abdomen of the volunteer and was fixated using a belt after a stable heart signal was found. For each volunteer, 2 min of Doppler signal and corresponding generated gating signal were recorded using an internal secure digital (SD) card. The stored Doppler signal was evaluated manually in order to validate the generated gating signals of the DUS device. The peaks were subsequently selected based on a visual assessment by two independent observers and compared to the gating signal generated by the DUS device.

Fetal MRI

To evaluate the DUS gating device, one volunteer (34 gestational weeks) was examined at 1.5T (Achieva; Philips Medical Systems Best, the Netherlands) and one volunteer (36 gestational weeks) at 3T (Ingenia; Philips Medical Systems). The developed DUS device was approved by the local ethics committee. For fetal cardiac cine imaging, gating signals were acquired with the MRI-conditional DUS device and transferred to the physiologic unit of the MRI scanner in real-time. For each scan, the transducer was placed above the fetal heart and fixated using a belt. Retrospectively gated cine balanced SSFP sequences were acquired in four-chamber view for 1.5T (pixel spacing = 1.0 × 1.0 mm^2, slice thickness = 5 mm, TR = 5.0 ms, TE = 1.6 ms, flip-angle = 60°, parallel acquisition technique = SENSE (acceleration factor = 2), matrix = 288 × 288, phases = 20, slices = 1, temporal resolution = 30 ms, acquisition duration = 9 s) and 3T (pixel spacing = 1.0 × 1.0 mm^2, slice thickness = 5 mm, TR = 5.0 ms, TE = 1.6 ms, flip-angle = 60°, parallel acquisition technique = SENSE (acceleration factor = 2), matrix = 288 × 288, phases = 20, slices = 1, temporal resolution = 30 ms, acquisition duration = 9 s). Gating signals were stored during data acquisition and analyzed with respect to gating quality and variability. Fetal cardiac cine images were analyzed in terms of endocardial blurring.

Results

MRI safety evaluation

The ability to attenuate common mode currents on the cable shield was measured for each cable trap at the desired Larmor frequency of 64 and 128 MHz (Table 1). Each cable trap fulfilled the requirement of at least 20 dB attenuation. Gradient echo images with the transducer and transmission line between the phantoms are shown in Fig. 3. B_1 image homogeneity showed no visible distortion within the whole phantom. Measurements of the mean flip angle showed a mean difference between images with and without transmission line of 4.9 ± 18% at 3T and of 6.5 ± 1.2% at 1.5T (Fig. 3). It can be seen that the transmission line is not affecting the image homogeneity and signal intensity, indicating a successful suppression of shield currents. The maximum difference in signal intensity of the gradient echo images between the two phantoms with and without transmission line was 4% for 1.5T and 6% for 3T.

Evaluation using a fetal cardiac phantom

The fetal cardiac phantom was successfully evaluated at 1.5T and 3T without image artifacts (Fig. 4). The contraction of the fetal heart phantom could be clearly visualized from systole to diastole at 1.5T and 3T without motion artifacts with a good delineation of the simulated ventricular walls (Fig. 4). The trigger generated by the DUS device during MRI was derived without distortions due to electromagnetic interferences and showed a high correlation to the simultaneously acquired control signal of $R = 0.99$ for 1.5T and $R = 0.99$ for 3T, respectively. A total of 2924 heart cycles were acquired at 1.5T and 2789 heart cycles at 3T, whereas the DUS device was able to detect all generated heart cycles at 1.5T (100%), as well as at 3T (100%) (Table 2). The mean difference in RR cycle length between the control signal generated by the phantom and the DUS gating signal was 5.5 ± 4.5 ms for 1.5T and 5.6 ± 4.6 ms for 3T, respectively. The control signal showed a variability of 0.1 ± 0.01 ms. The detected heart cycle by the DUS device showed an increased variability of 6.4 ± 2.1 ms for 1.5T and 6.5 ± 2.9 ms for 3T. The mean correlation for the combined data of detected trigger time points of 1.5T and 3T measurements in comparison to the control signal generated by the heart phantom was $R = 0.99$ with a mean offset of 4.1 ± 2.3 ms (Fig. 5).

Table 1 Results of cable trap attenuation

Cable trap	1	2	3	4
64 MHz (S21 dB)	48	50	47	45
128 MHz (S21 dB)	42.42	47.18	39.15	26.22

The values shown in the table are the S21 measurement results in dB for each cable trap at 1.5T (64 MHz) and 128 MHz (3T) using a network analyzer and current probes. Each cable trap fulfilled the minimum requirement of 20 dB.

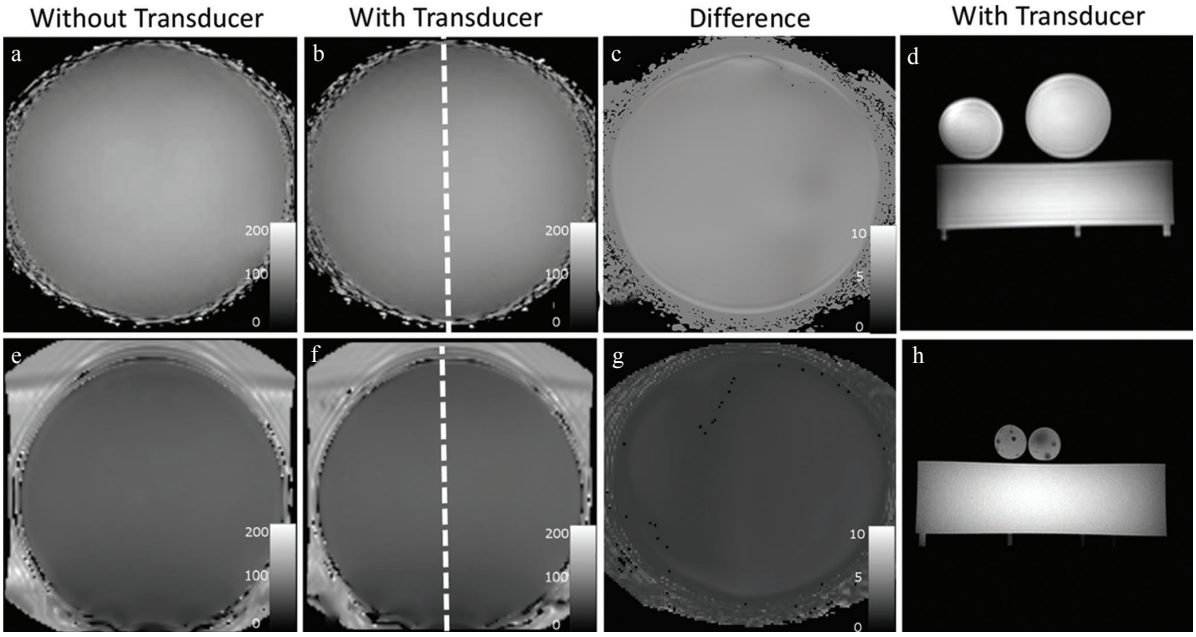

Fig. 3 Shown are coronal B_1 flip angle maps and axial gradient echo images at 1.5T (upper row) and at 3T (bottom row) for cases with transducer inside the scanner (dashed line) on top of the phantom in (**b**) and (**f**) and without transducer inside the magnetic resonance scanner in (**a**) and (**e**). No effects on B_1 field homogeneity due to the cable or transducer are visible for 1.5T or for 3T as shown in the image difference in (**c**) and (**g**). No geometric distortions or signal loss due to common-mode currents were visible with the transducer inside the MRI using Gradient echo images for 1.5T (**d**) and for 3T (**h**).

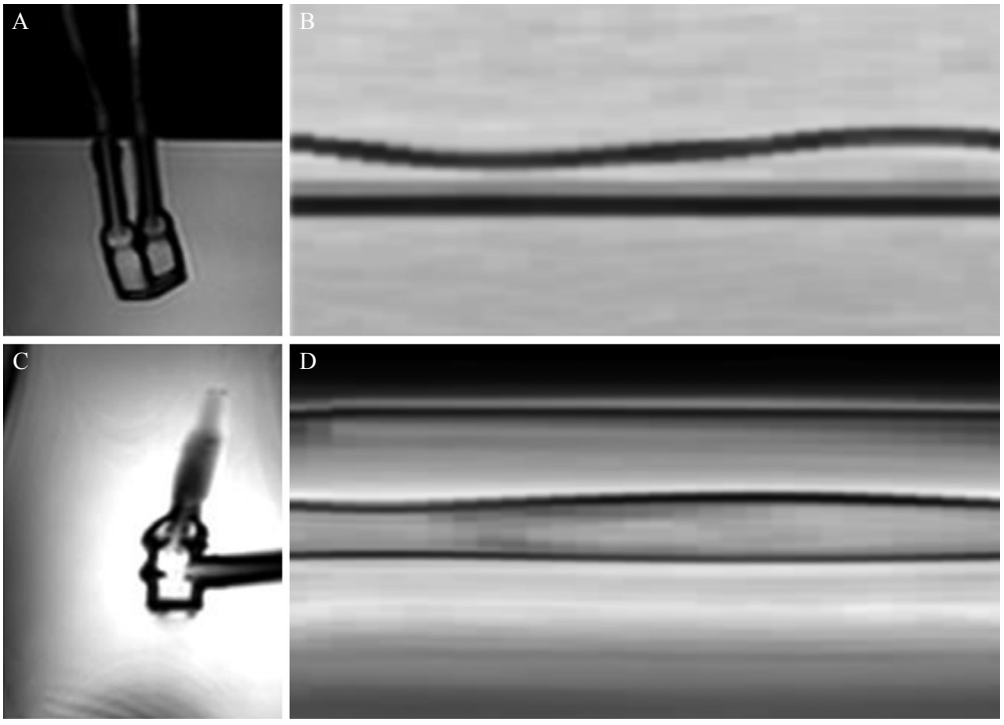

Fig. 4 Shown are exemplary steady-state free precession (SSFP) images of the fetal cardiac phantom at 1.5T (upper row) and at 3T (bottom row). Images during mid-diastole are shown in (**a**) and in (**c**) with their corresponding projection over one whole cardiac cycle in (**b**) and (**d**).

Verification of the DUS algorithm

Mean results for all volunteers are shown in Table 2. A total of 3876 heart cycles were evaluated whereas the DUS device detected 3860 heart cycles with a sensitivity compared to the manually selected heart cycles of 99%. The mean RR length of manually selected heart cycles was 434 ± 32 ms and the mean RR length of detected trigger time points by the DUS device was 434 ± 31 ms.

Table 2 DUS gating results

		RR intervals	RR length (ms)	Difference in RR length (msec)	Variability (msec)	Sensitivity (%)
1.5T	Heart phantom	2924	408 ± 127	–	0.1 ± 0.01	100
	DUS device	2924	404 ± 126	5.5 ± 4.5	6.4 ± 2.1	100
3T	Heart phantom	2789	444 ± 147	–	0.1 ± 0.01	100
	DUS device	2789	443 ± 147	5.6 ± 4.6	6.5 ± 2.8	100
Fetal verification	Heart cycle	1876	434 ± 32	–	22.0 ± 7.6	100
	DUS device	1860	434 ± 31	0.01 ± 11	22.2 ± 7.1	99.1

The values shown in the tables are the Doppler ultrasound (DUS) gating results for the phantom study at 1.5T and 3T and for the *in vivo* verification study outside the MRI room. RR, beat-to-beat.

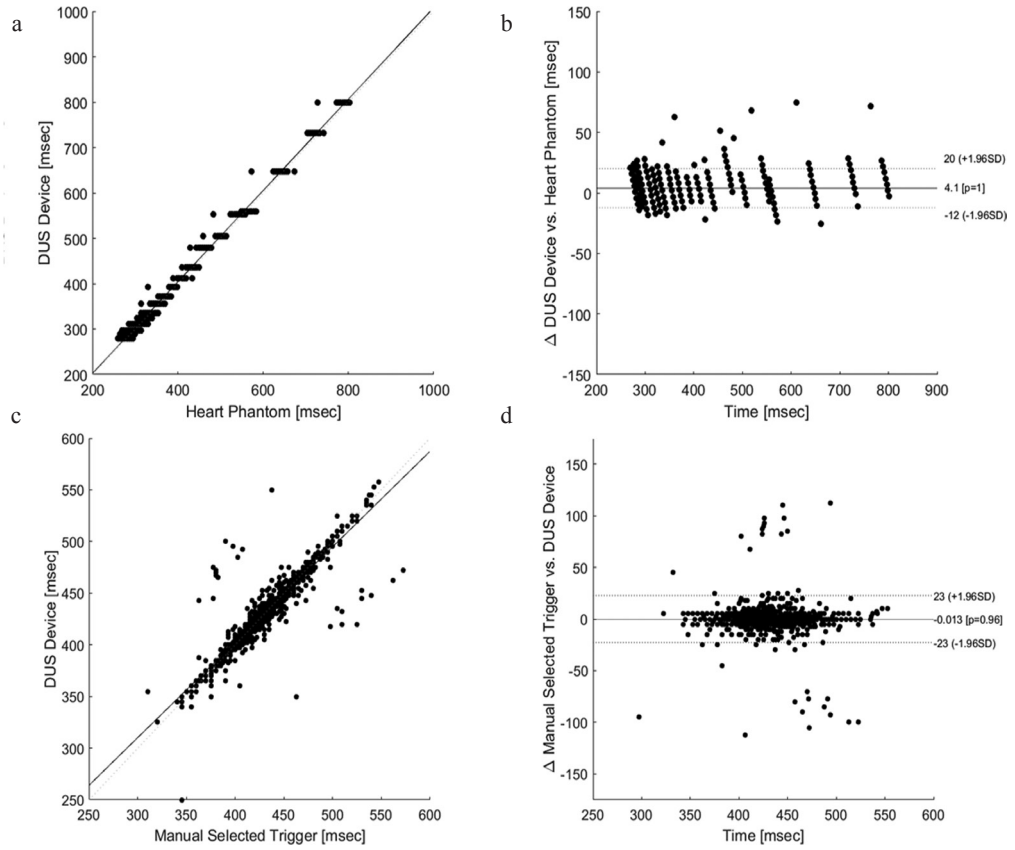

Fig. 5 The results of the Doppler ultrasound (DUS) gating validation using the heart phantom during MRI acquisition for heart rates ranging from 75 to 200 BPM is shown in (**a**) and (**b**), for the *in vivo* validation outside of MRI in (**c**) and (**d**). The dashed lines of the Bland Altman plot in (**b**) and (**d**) represent the confidence interval of ±1.96 of the standard deviation.

The variability of the gating signal and the manually selected heart cycle was 22.0 ± 7.6 ms and 22.0 ± 7.6 ms, respectively. The correlation between the DUS gating signal and the manually selected heart cycles was $R = 0.99$ with a mean difference of 0.1 ± 11 ms (Fig. 5).

Fetal MRI

Fetal cardiac MRI was possible at 1.5T and 3T using the external gating signal provided by the DUS device. The DUS signal was stable throughout all measurements and no repositioning was necessary whereas each examination was completed after approximately 35 min. The DUS signals recorded during MR cine imaging were not influenced by electromagnetic interferences and showed no artifacts as exemplarily shown in Fig. 6 for 1.5T. For cine imaging at a total of 37 RR intervals were acquired at 1.5T and 65 intervals at 3T with a mean RR length of 395 ± 22 ms and 475 ± 34 ms, respectively. A total of four intervals (1.5T) and one interval (3T) were excluded by the MRI scanner due to arrhythmia, resulting in a sensitivity of 90% and 99%, respectively. Retrospectively gated cardiac cine images of the fetus are shown in Fig. 7 for 1.5T and 3T with corresponding M-mode projection over one entire cardiac cycle calculated in a mid-ventricular position in the four-chamber view. Indicating correct gating, the contraction of the heart was clearly visible from the apex to the base, whereas the atrial septum could be clearly depicted without motion artifacts.

Discussion

An MRI conditional and portable DUS device was successfully developed and evaluated for 1.5T and 3T in terms of MR compatibility, functionality, and reliability. It was shown that the DUS device is MR conditional and can be operated within the MRI without being influenced by electromagnetic interferences. The feasibility to detect the fetal heart motion and to generate a trigger signal was confirmed in a validation study of fetuses outside the MRI room. In addition, the device was successfully applied in a preliminary test for fetal cardiac cine imaging at 1.5T and 3T without motion artifacts and good delineation of ventricular motion.

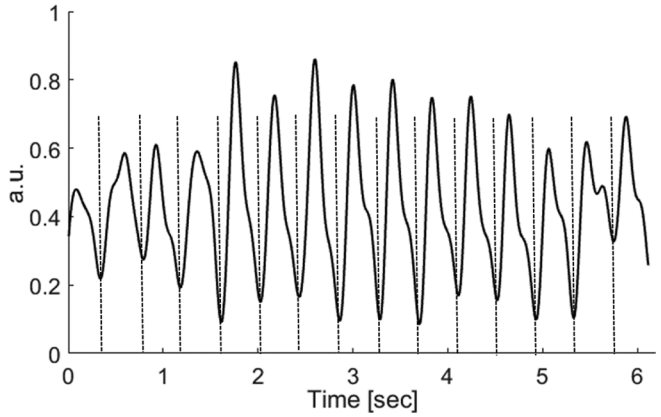

Fig. 6 Exemplary the Doppler ultrasound (DUS) signal during MRI acquisition for one fetus at 1.5T. The dashed lines represent the detected gating time points of DUS device which are sent to the physiologic unit of the MRI scanner for gating.

One prerequisite for cardiac cine MRI is accurate synchronization with the cardiac cycle.[11] As the heart cycle and hence the gating signal of the fetal heart cannot be derived within the MRI environment employing the routinely used electrocardiogram,[14] a different technique was developed in this work based on DUS. The DUS is routinely used in obstetrics for fetal heart rate monitoring[28,29] and is an ideal method to derive the fetal heart rate as the method is theoretically not influenced by the electromagnetic field of the MRI[17,18,30] and hence promises a stable gating signal. Although ultrasound is not interacting with electromagnetic fields, a cable and piezoelectric elements are still necessary for signal transmission, which can couple significantly with the RF transmit field of the MRI. As the used cable is longer than the free-space wavelength, common mode signals cannot be ignored as local electric field amplifications can lead to a potentially large temperature increase along the cable.[31–33] This circumstance significantly influences patients' safety and MRI signal reception. In order to reduce the risk of an RF burn of the patient and to reduce excessive noise in the MRI signal, cable traps[22,23,34] were chosen to prevent common mode currents on the cable shield. The suppression of common mode currents for each cable trap should provide an attenuation of at least 20 dB in order to provide an effective protection against an unwanted temperature increase and related effects such as MRI signal loss.[35] It was shown that each trap used in this work complies with the requirement using a standard network analyzer. Moreover, interactions of the transducer and the cable with the electromagnetic field of the MRI were evaluated in detail. If common mode currents are present on the cable shield, the image homogeneity will be affected as

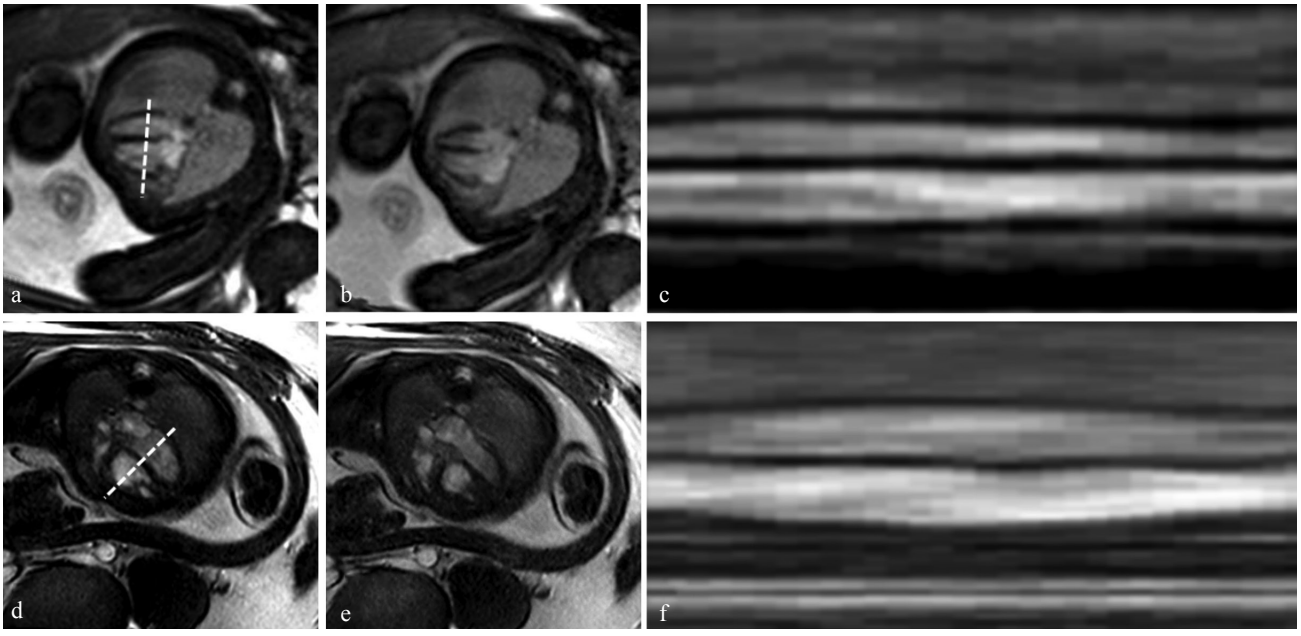

Fig. 7 Preliminary fetal cardiac steady-state free precession (SSFP) cine images in four-chamber view for 1.5T (upper row) and 3T (bottom row). Gated images are shown in diastole in (**a**) and (**d**), for systole in (**b**) and (**e**). The corresponding projection over one cardiac cycle is shown in (**c**) and (**f**).

shown by Seeber et al.,[23] resulting in a decreased signal intensity. It was shown that the introduction of the cable and transducer did not affect the signal intensity. The maximum change was in the order of reported values of 2–6% by Seeber et al.,[23] indicating a sufficient attenuation of common mode signals. Moreover, common mode signals on the cable shield take on characteristics of antennas and will influence the B_1 field.[35] It was shown in this work that the B_1 field is not altered, indicating a correct attenuation of common mode signals. As the measurements at the test bench and inside the MRI showed a concurrent suppression of common mode signals, the cable and transducer were considered MR conditional.

In addition to the required MRI safety, the DUS device was evaluated regarding possible distortions due to MRI interferences. The results using the heart phantom showed no interaction between the MRI and the DUS signal and a high correlation between the generated motion of the heart phantom and DUS gating signal over a wide range of different heart rates for both evaluated field strengths. The DUS device showed a very high sensitivity where no heart cycle was missed at both field strength. Moreover, the DUS signal and MRI images showed no artifacts in the DUS or MRI signal, hence indicating a sufficient MRI compatibility for 1.5T and 3T. The variability of the detected heart motion was in the order of 5.5 ms. However, the detection is dependent on the movement of the heart, the correct detection by the algorithm, processing time and by the sampling rate of the system. As the sampling rate was 200 Hz, the variability of the generated gating signal will automatically vary about 5 ms. Hence, the added variability added by the DUS device was less than 1 ms and therewith negligible compared to the heart rate variability of the fetal heart, which is in the order of 25 ms.[36]

Besides the prerequisite of MRI compatibility, the DUS device should reliably detect the fetal heart movement. Hence, the developed system and algorithm was evaluated *in vivo* in healthy pregnant volunteers outside the MR environment, comparing DUS detected and manually selected heart cycles. In accordance with results of the heart phantom, the measurements showed a high correlation between detected heart cycles by the DUS device and the manually selected heart cycles. One of the main requirements for the DUS device is an accurate detection of the heart cycle with a low variability as a high variability in trigger time points leads to image blurring.[20,37] In this work, the measured heart rate variability is in the range of previously reported values of 16–25 ms[38] indicating an accurate detection of each heart cycle.

As the DUS device showed sufficient MRI compatibility and functionality in terms of safety and accurate heart rate detection, it was used for fetal cardiac cine imaging at 1.5T and 3T MRI systems in a preliminary test. Images were acquired in four-chamber view as it is the most important view regarding a number of congenital heart diseases that have a change in ventricular size.[39] Acquisition of cine images was successful at 1.5T and 3T and showed no motion artifacts related to incorrect gating. The contraction of the fetal ventricles was clearly visible without artifacts in each of the acquired heart phases, which is important for the evaluation of fetal morphology and diagnosis of e.g., hypoplastic left heart syndrome or tricuspid atresia.

The scope of this work was the development and evaluation of the DUS device in terms of MR compatibility and functionality. It was shown that the DUS device is not altered by the electromagnetic field of the MRI and that the device shows a sufficient MR compatibility in order to provide patient safety. As fetal cardiac MRI has the potential to become an important diagnostic tool for diagnosis of fetal congenital abnormalities in addition to fetal echocardiography,[12,13,39] the ability to evaluate the fetal cardiac kinetics will become more important.

To overcome the current limitation of no available gating method for fetal cardiac MRI several methods were introduced in the past based on post-processing. One major innovation was the introduction of metric optimized gating, which is based on an iterative process to optimize the image metric until the correct heart rate or minimal motion blurring is found.[14,40] In addition, metric optimized gating was recently combined with compressed sensing and radial undersampling to overcome fetal body motion during acquisition.[41] Other post-processing methods are also based on retrospective processing to detect motion and to correct for its effect.[12,13] Although post-processing techniques have the advantage of not utilizing additional hardware and are able to produce high-quality diagnostic images, post-processing times of up to 2 h for a single slice illustrate the current limitation of all such techniques for the implementation in clinical routine.[40] Currently used post-processing methods are designed to reveal the fetal heart rate in order to correct for image blurring. One major advantage of a direct gating method is an immediate reconstruction, allowing adjustments of imaging planes and assessment of image quality during examination. Moreover, a direct gating signal allows the application of clinically used cardiac MRI sequences and methods, such as cine SSFP and phase contrast imaging for fetal cardiac MRI.

This work should provide the basis for future studies that have to investigate the feasibility of DUS gated fetal cardiac MRI in a larger cohort with a special focus on image quality and analysis of cardiac anatomical structures.

One limitation of the DUS device is that it cannot adjust for major fetal body motion. If the fetal heart moves out of the acoustic field of the DUS transducer, the DUS signal will be lost and no gating signal can be produced. However, the coverage of the acoustic field of the DUS transducer has a diameter of 6 cm and any motion within this range leads to a stable trigger signal. One possibility to adapt for major fetal motion could be the usage of multiple transducers or an increase of the acoustic field. Moreover, another limitation is that the DUS device was only validated in healthy fetuses outside the MR environment in order to verify the developed algorithm. The detection of one heart cycle could be influenced in cases of congenital heart diseases, such as complex

malformations. Hence, the signal quality of the DUS device for cardiac gating needs further evaluation to ensure reliable gating signals for pathological conditions. Feasibility of the DUS device to perform dynamic fetal cardiac MRI and image quality have to be evaluated in future studies.

Conclusion

In conclusion, the DUS device showed a sufficient MR compatibility for 1.5T and 3T and was validated successfully outside the MRI room and in a phantom study without being influenced by the electromagnetic field of the MRI and without introducing image artifacts. It was shown that an accurate gating can be provided in real time during MRI image acquisition using DUS, without extensive and time-consuming post-processing techniques. Preliminary results of a fetal cardiac MR examination at 1.5T and 3T revealed that the DUS device has the potential to realize dynamic fetal cardiac MRI. However, in future studies, this method has to be applied in a larger study group to confirm feasibility and to investigate the image quality and diagnostic potential.

Acknowledgment

This study was supported by a grant of the German Research Foundation, SCHO1564/1-1 (DFG).

Conflicts of Interest

The authors C. Ruprecht, K. Fehrs, and F. Kording are inventor and shareholder of the pending patent WO 2017/102924 A1 "Ultrasonic Device for Detecting the Heartbeat of a Patient". No money has been paid to any of the authors or the related institutions.

References

1. Allan L. Technique of fetal echocardiography. Pediatr Cardiol 2004; 25:223–233.
2. Hunter LE, Simpson JM. Prenatal screening for structural congenital heart disease. Nat Rev Cardiol 2014; 11:323–334.
3. Wielandner A, Mlczoch E, Prayer D, Berger-Kulemann V. Potential of magnetic resonance for imaging the fetal heart. Semin Fetal Neonatal Med 2013; 18:286–297.
4. Forbus GA, Atz AM, Shirali GS. Implications and limitations of an abnormal fetal echocardiogram. Am J Cardiol 2004; 94:688–689.
5. Levi S. Ultrasound in prenatal diagnosis: polemics around routine ultrasound screening for second trimester fetal malformations. Prenat Diagn 2002; 22:285–295.
6. Bensemlali M, Stirnemann J, Le Bidois J, et al. Discordances between pre-natal and post-natal diagnoses of congenital heart diseases and impact on care strategies. J Am Coll Cardiol 2016; 68:921–930.
7. Rutherford M, Jiang S, Allsop J, et al. MR imaging methods for assessing fetal brain development. Dev Neurobiol 2008; 68:700–711.
8. Prakash A, Powell AJ, Geva T. Multimodality noninvasive imaging for assessment of congenital heart disease. Circ Cardiovasc Imaging 2010; 3:112–125.
9. Head CEG, Jowett VC, Sharland GK, Simpson JM. Timing of presentation and postnatal outcome of infants suspected of having coarctation of the aorta during fetal life. Heart 2005; 91:1070–1074.
10. Lloyd DF, van Amerom JF, Pushparajah K, et al. An exploration of the potential utility of fetal cardiovascular MRI as an adjunct to fetal echocardiography. Prenat Diagn 2016; 36:916–925.
11. Chia JM, Fischer SE, Wickline SA, Lorenz CH. Performance of QRS detection for cardiac magnetic resonance imaging with a novel vectorcardiographic triggering method. J Magn Reson Imaging 2000; 12:678–688.
12. Haris K, Hedström E, Bidhult S, et al. Self-gated fetal cardiac MRI with tiny golden angle iGRASP: a feasibility study. J Magn Reson Imaging 2017: 46:207–217.
13. van Amerom JFP, Lloyd DFA, Price AN, et al. Fetal cardiac cine imaging using highly accelerated dynamic MRI with retrospective motion correction and outlier rejection. Magn Reson Med 2018; 79:327–338.
14. Roy CW, Seed M, Macgowan CK. Accelerated MRI of the fetal heart using compressed sensing and metric optimized gating. Magn Reson Med 2017; 77:2125–2135.
15. Tuck DL. Improved Doppler ultrasonic monitoring of the foetal heart rate. Med Biol Eng Comput 1981; 19: 135–140.
16. Feinberg DA, Günther M. Simultaneous MR and ultrasound imaging: towards US-navigated MRI. Proceedings of the 11th Annual Meeting of ISMRM, Toronto, 2003; 381.
17. Feinberg DA, Giese D, Bongers DA, et al. Hybrid ultrasound MRI for improved cardiac imaging and real-time respiration control. Magn Reson Med 2010; 63:290–296.
18. Günther M, Feinberg DA. Ultrasound-guided MRI: preliminary results using a motion phantom. Magn Reson Med 2004; 52:27–32.
19. Kording F, Yamamura J, Lund G, et al. Doppler ultrasound triggering for cardiovascular MRI at 3T in a healthy volunteer study. Magn Reson Med Sci 2017; 16:98–108.
20. Kording F, Schoennagel B, Lund G, et al. Doppler ultrasound compared with electrocardiogram and pulse oximetry cardiac triggering: a pilot study. Magn Reson Med 2015; 74:1257–1265.
21. Yamamura J, Kopp I, Frisch M, et al. Cardiac MRI of the fetal heart using a novel triggering method: initial results in an animal model. J Magn Reson Imaging 2012; 35:1071–1076.
22. Peterson DM, Beck BL, Duensing GR, Fitzsimmons JR. Common mode signal rejection methods for MRI: Reduction of cable shield currents for high static magnetic field systems. Concepts Magn Reson part B: Magn Reson Eng 2003; 19:1–8.
23. Seeber DA, Jevtic J, Menon A. Floating shield current suppression trap. Concepts Magn Reson Part B: Magn Reson Eng 2004; 21B:26–31.
24. Szabo T. Diagnostic ultrasound imaging: inside out. Elsevier. second edition. Burlington, MA, London; Academic Press; 2003.
25. Loushin MK, Quill JL, Iaizzo PA. Mechanical aspects of cardiac performance. In: Iaizzo PA. Handbook of Cardiac

Anatomy, Physiology, and Devices. Switzerland: Springer; 2015. 335–360.
26. Hardy PT, Weil KM. A review of thermal MR injuries. Radiol Technol 2010; 81:606–609.
27. Oberhoffer R, Högel J, Lang D. Normal characteristics of cardiac dimensions and function in the fetus. Eur J Ultrasound 1995; 2:93–106.
28. Peters CH, ten Broeke ED, Andriessen P, et al. Beat-to-beat detection of fetal heart rate: Doppler ultrasound cardiotocography compared to direct ECG cardiotocography in time and frequency domain. Physiol Meas 2004; 25:585–593.
29. Jezewski J, Roj D, Wrobel J, Horoba K. A novel technique for fetal heart rate estimation from Doppler ultrasound signal. Biomed Eng Online 2011; 10:92.
30. Petrusca L, Cattin P, De Luca V, et al. Hybrid ultrasound/magnetic resonance simultaneous acquisition and image fusion for motion monitoring in the upper abdomen. Invest Radiol 2013; 48:333–340.
31. Nordbeck P, Fidler F, Weiss I, et al. Spatial distribution of RF-induced E-fields and implant heating in MRI. Magn Reson Med 2008; 60:312–319.
32. Luechinger R, Zeijlemaker VA, Pedersen EM, et al. In vivo heating of pacemaker leads during magnetic resonance imaging. Eur Heart J 2005; 26:376–383; discussion 325–327.
33. Kugel H, Bremer C, Püschel M, et al. Hazardous situation in the MR bore: induction in ECG leads causes fire. Eur Radiol 2003; 13:690–694.
34. Ladd ME, Quick HH. Reduction of resonant RF heating in intravascular catheters using coaxial chokes. Magn Reson Med 2000; 43:615–619.
35. Vaughan JT, Griffiths JR. RF coils for MRI. Hoboken, NJ, USA: John Wiley & Sons, Inc.; 2012.
36. De Haan J, Van Bemmel JH, Versteeg B, et al. Quantitative evaluation of fetal heart rate patterns: I. Processing methods. Eur J Obstet Gynecol 1971; 1:95–102.
37. Frauenrath T, Hezel F, Renz W, et al. Acoustic cardiac triggering: a practical solution for synchronization and gating of cardiovascular magnetic resonance at 7 Tesla. J Cardiovasc Magn Reson 2010; 12:67.
38. Jeiewski J, Wrobel J. Fetal monitoring with automated analysis of cardiotocogram: the Kompor system. Engineering in Medicine and Biology Society, 1993. Proceedings of the 15th Annual International Conference of the IEEE, IEEE; 1993;638–639.
39. Dong SZ, Zhu M, Li F. Preliminary experience with cardiovascular magnetic resonance in evaluation of fetal cardiovascular anomalies. J Cardiovasc Magn Reson 2013; 15:40.
40. Roy CW, Seed M, van Amerom JF, et al. Dynamic imaging of the fetal heart using metric optimized gating. Magn Reson Med 2013; 70:1598–1607.
41. Roy CW, Seed M, Kingdom JC, Macgowan CK. Motion compensated cine CMR of the fetal heart using radial undersampling and compressed sensing. J Cardiovasc Magn Reson 2017; 19:29.